Journal of Materials Chemistry C

PAPER

View Article Online
View Journal | View Issue

Cite this: J. Mater. Chem. C, 2014, 2, 319

Liquid crystalline radicals: discotic behavior of unsymmetrical derivatives of 1,3,5-triphenyl-6-oxoverdazyl†

Aleksandra Jankowiak,[a] Damian Pociecha,[b] Jacek Szczytko,[c] Hirosato Monobe[d] and Piotr Kaszyński*[ae]

Received 9th October 2013
Accepted 23rd October 2013

DOI: 10.1039/c3tc31984a

www.rsc.org/MaterialsC

A series of six 6-oxoverdazyl (**1[10]**) substituted with a total of three 3,4,5-tri(decyloxy)phenyl and/or 3,4,5-tri(decylsulfanyl)phenyl groups was investigated by thermal, XRD, spectroscopic, magnetic and photovoltaic methods. The compounds exhibit columnar hexagonal (**1[10]c**, Col_h), columnar hexagonal ordered (**1[10]b**, $Col_{h(o)}$), columnar hexagonal 3D (**1[10]a**, **1[10]e** and **1[10]f**, $Col_{h(3D)}$) or a sequence of two phases (**1[10]b**, Col_h–$Col_{h(3D)}$). The mesophase structure and stability and also thermochromism were investigated as a function of the number and distribution of decyloxy and decylsulfanyl substituents in the molecule. Thermal analysis demonstrated that the presence of the 3,4,5-tri(decyloxy)phenyl substituent in the C(3) position increases the phase stability. Spectroscopic analysis showed that only all-decyloxy derivative **1[10]b** exhibits a hypsochromic shift upon $Col_{h(o)}$ formation, while all other compounds in the series show a modest bathochromic shift in the columnar phase relative to the isotropic phase. Magnetization investigation of **1[10]d** demonstrated the paramagnetic behavior of isolated spins in isotropic and columnar phases. Negligible photocurrent was detected for **1[10]d** in the columnar phase.

Introduction

Liquid crystalline radicals with π-delocalized electron spins[1] constitute an emerging class of materials for fundamental studies of spin–spin interactions in supramolecular assemblies and potential applications as organic semiconductors.[2–5] In this context, we have focused on the verdazyl as a centerpiece of mesogenic compounds,[2–4,6] and recently reported two series of discotic derivatives **1[*n*]a** and **1[*n*]b** (Chart 1). The former series,[2,6] 1,3,5-tris(3,4,5-trialkylsulfanylphenyl)-6-oxoverdazyls (**1[*n*]a**, $n = 6$, 8, 10), exhibits a 3-dimensional columnar hexagonal phase ($Col_{h(3D)}$)[6] below 60 °C and a broad absorption band in the visible range resulting in a dark blue-violet color. In contrast, the alkoxy analogues **1[*n*]b** form a broad-range ordered columnar hexagonal phase ($Col_{h(o)}$) with clearing temperatures below 130 °C, and exhibit a pronounced thermochromism: in the isotropic phase they are dark green, while in the discotic phase they become red.[3] In both series of compounds photocurrent was detected, and the hole mobility μ_h was foundc3tc31984a-f to be in the order of 10^{-3} cm^2 V^{-1} s^{-1} in the mesophase.[2,3]

Tuning of properties, such as the type, range and stability of the mesophase and thermochromism, in this class of discogens could be achieved by "combining" aryl fragments from each of the series. For this purpose we chose the symmetric derivatives **1[10]a** and **1[10]b** and prepared analogous "mixed" derivatives containing both the 3,4,5-tri(decylsulfanyl)phenyl and 3,4,5-tri(decyloxy)phenyl substituents. Here we report four "mixed" derivatives **1[10]c**–**1[10]f** (Chart 1) and analyze structural effects

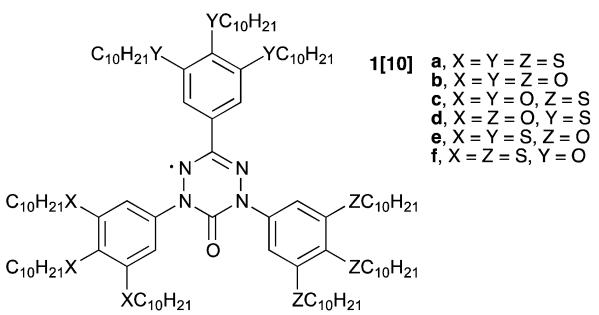

Chart 1

[a]Organic Materials Research Group, Department of Chemistry, Vanderbilt University, Nashville, TN 37235, USA. E-mail: piotr.kaszynski@vanderbilt.edu.
[b]Department of Chemistry, University of Warsaw, Żwirki i Wigury 101, 02-089 Warsaw, Poland
[c]Institute of Experimental Physics, Faculty of Physics, University of Warsaw, Hoża 69, 00-681 Warsaw, Poland
[d]Research Institute for Ubiquitous Energy Devices, National Institute of Advanced Industrial Science and Technology, AIST Kansai Centre, Ikeda, Osaka 563-8577, Japan
[e]Faculty of Chemistry, University of Łódź, Tamka 12, 91403 Łódź, Poland

† Electronic supplementary information (ESI) available: Additional synthetic details and characterization data for intermediates **4[10]**–**6[10]**, XRD details, α-FMO contours, partial TD-DFT output, and an archive of calculated equilibrium geometries for **1[1]** and **7**. See DOI: 10.1039/c3tc31984a

on the mesophase and electronic absorption. We also investigate the derivative **1[10]d** for its magnetic and photovoltaic properties.

Results and discussion

Synthesis

Synthesis of radicals **1[10]** follows the Milcent method[7] used previously for the preparation of **1[*n*]a** and **1[*n*]b** (Scheme 1). Thus, a reaction of appropriate hydrazine **2[10]**[8] and benzaldehyde **3[10]**[9] gave crude hydrazone **4[10]**, which upon treatment with triphosgene yielded carbonyl chloride **5[10]**. After isolation and purification, the chloride was reacted with hydrazine **2[10]** in benzene. The resulting tetrazine **6[10]** was partially purified and oxidized with PbO_2 to give radical **1[10]** in 5–15% overall yield.

Electronic absorption

Hexane solutions of all radicals **1[10]** exhibit low intensity broad absorption bands in the visible range with maxima at about 610 nm and 500 nm (Fig. 1). The UV portion of the spectra exhibits absorption bands characteristic of the 3,4,5-trialkylsulfanylphenyl (~260 nm) and 3,4,5-trialkoxyphenyl (~210 nm) groups. According to TD-DFT results for models **1[1]**, the low energy absorption bands originate from several $\pi \rightarrow \pi^*$ electronic transitions that involve 5 highest occupied β MOs, localized mostly on the benzene rings, to the β-LUMO, localized solely on the verdazyl unit, as shown for **1[1]c** in Fig. 2. The lowest energy excitations at about 600 nm have a small contribution from the SOMO (α-HOMO) to the α-LUMO transition, in which both orbitals are associated with the verdazyl unit.[10] Further analysis revealed that the verdazyl unit contains the bulk spin density and little is delocalized into benzene rings (Fig. 3) in agreement with other results for verdazyls.[11]

Thermal analysis

Analysis of compounds in series **1[10]** by thermal (DSC) and optical methods (POM) demonstrated that all exhibit liquid crystalline behavior (Table 1). The most stable mesophase was found for the tris(3,4,5-tridecyloxyphenyl) derivative **1[10]b**, for which the $Col_{h(o)}$ phase becomes isotropic at 121 °C.[3] Replacement of the aryl substituent at the N(1) position of **1[10]b** with the 3,4,5-tri(decylsulfanyl)phenyl group in **1[10]c** destabilized the mesophase by 30 K and eliminated the ordered

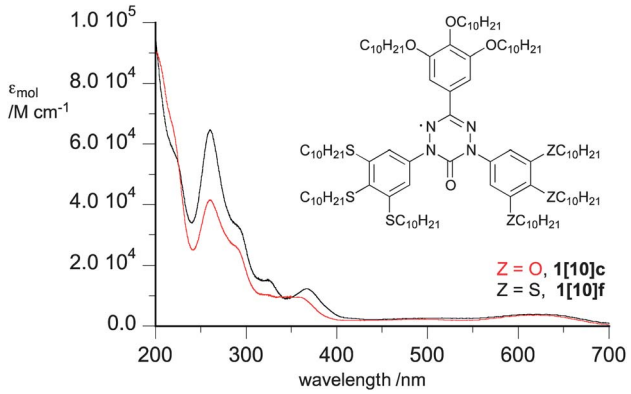

Fig. 1 Electronic absorption spectra of **1[10]c** (red) and **1[10]f** (black) in hexane.

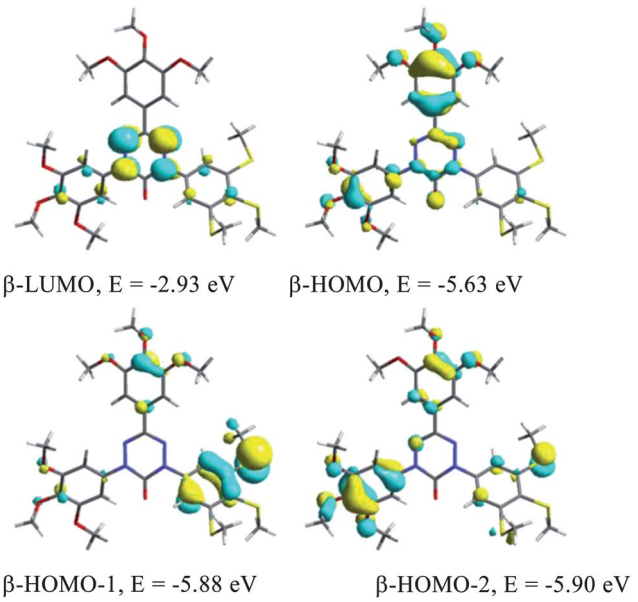

Fig. 2 B3LYP/6-31G(d,p) derived contours and energies of β-FMOs involved in low energy excitations in **1[1]c**.

character of the columnar phase, as evident from XRD analysis (*vide infra*). The texture of the mesophase, containing pseudoisotropic areas with only a few birefringent domains (*e.g.* Fig. 4a) is typical for columnar hexagonal phases. Interestingly, the

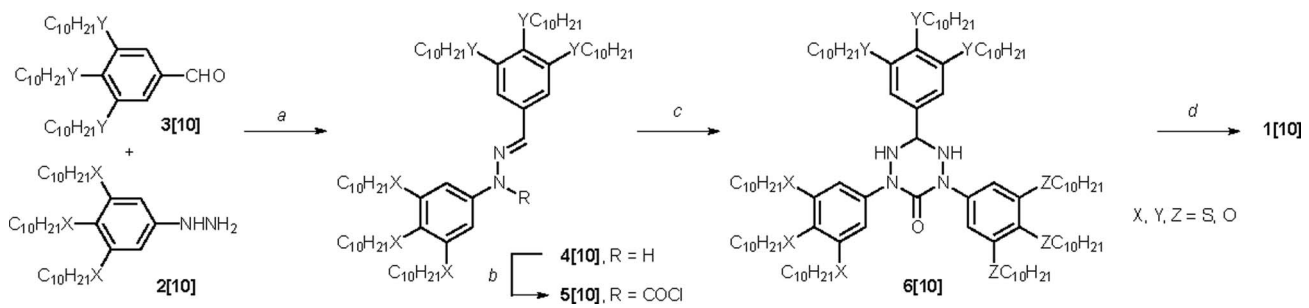

Scheme 1 *Reagents and conditions*: (a) EtOH, cat. AcOH, reflux; (b) $CO(OCCl_3)_2$, pyridine, CH_2Cl_2, rt; (c) **2[10]**, Et_3N, benzene, 50 °C; (d) PbO_2, Na_2CO_3, toluene/MeCN.

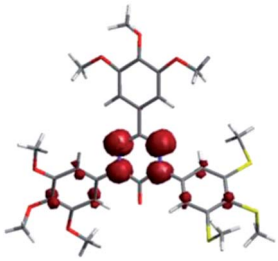

Fig. 3 B3LYP/6-31G(d,p) derived total spin density in **1[1]c**.

Table 1 Transition temperatures [°C] and enthalpies [kJ mol^{-1}] for **1[10]**[a]

1[10]	X	Y	Z	
a[b]	S	S	S	Cr 62 (125.6) ($Col_{h(3D)}$ 55 (14.0)) I
b[c]	O	O	O	Cr < $Col'_{h(o)}$ 20 (23.3) $Col_{h(o)}$ 121 (57.3) I
c	O	O	S	Cr[d] 47 (34.5) Col_h 91 (17.9) I
d	O	S	O	Cr 57 (81.0) $Col_{h(3D)}$ 78 Col_h 80 (19.7)[e] I
e	S	S	O	Cr 51 (109.3) $Col_{h(3D)}$ 67 (19.8) I
f	S	O	S	Cr 49 (136.8) $Col_{h(3D)}$ 102 (52.1) I

[a] Determined by DSC (5 K min^{-1}) in the heating mode: Cr = crystalline; Col_h = columnar hexagonal; $Col_{h(o)}$ = columnar hexagonal ordered; $Col_{h(3D)}$ = columnar hexagonal 3D; I = isotropic. [b] Ref. 2 and 6. [c] Ref. 3. [d] Cr–Cr at 39 °C (22.1 kJ mol^{-1}). [e] Combined enthalpy. Heating rate 2 K min^{-1}.

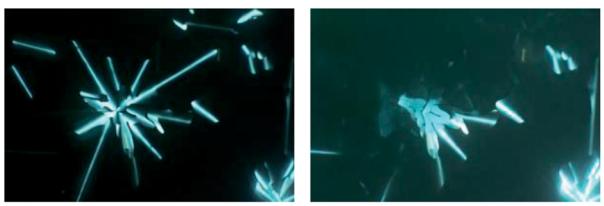

Fig. 4 Optical textures observed for **1[10]d** in the same region of the sample: (a) Col_h phase at 78 °C and (b) $Col_{h(3D)}$ phase at 70 °C. The exposure times are 1/8 s for (a) and 1/3 s for (b).

same substitution at the C(3) position of **1[10]b** has a more pronounced effect on the mesophase: the columnar mesophase in compound **1[10]d**, an isomer of **1[10]c**, has lower thermal stability at 11 K, and the $Col_{h(3D)}$ phase, characteristic of series **1[*n*]a**, is formed below the narrow range Col_h phase (Table 1 and Fig. 5). This is in agreement with the expectations that the $Col_{h(3D)}$ phase is more organized than the Col_h phase. Optical analysis of both phases in **1[10]d** shows that bright domains visible in the texture of the high temperature Col_h phase loose birefringence upon phase transition to the $Col_{h(3D)}$ phase (Fig. 4).

Substitution of two 3,4,5-tri(decylsulfanyl)phenyl groups and one 3,4,5-tri(decyloxy)phenyl group into the verdazyl core induces only the $Col_{h(3D)}$ phase in derivatives **1[10]e** and **1[10]f** (Table 1) for which two characteristic textures, obtained on slow and fast cooling from the isotropic phase, are shown in Fig. 6. Again, the mesophase of the isomer with the 3,4,5-tri(decyloxyl)phenyl group at the C(3) position of the verdazyl ring exhibits higher thermal stability.

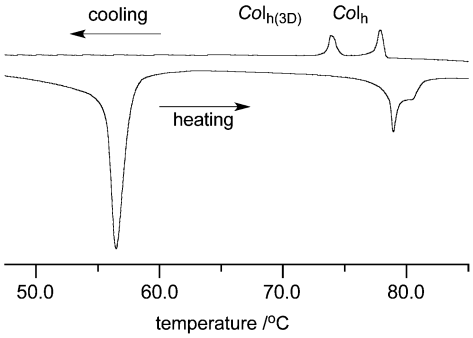

Fig. 5 DSC traces of **1[10]d**. The heating and cooling rates are 2 K min^{-1}.

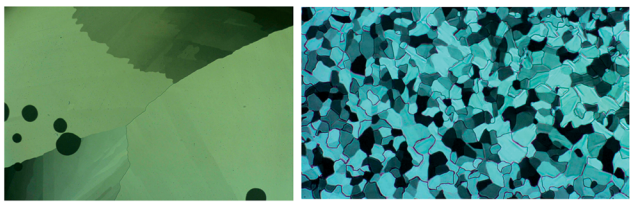

Fig. 6 Optical textures of a $Col_{h(3D)}$ phase obtained for **1[10]f** (a) by slow cooling from the isotropic phase to 90 °C, and (b) and by quenching the isotropic phase at ambient temperature.

Thus, the results demonstrate that derivatives **1[10]** with one 3,4,5-tri(decylsulfanyl)phenyl group exhibit the Col_h phase and with two such groups only the $Col_{h(3D)}$ phase is present. Also isomers with the 3,4,5-tri(decyloxy)phenyl group at the C(3) position have higher thermal stability; such derivatives are presumably more anisometric due to near coplanarity of two alkoxy substituents with the benzene ring and the whole aryl substituent with the central heterocycle (Fig. 2).

Thermochromism

Visible spectra were recorded for thin films of **1[10]** placed between glass slides in the isotropic phase and mesophase approximately 10 K away from the Col–Iso transition. Results shown in Table 2 demonstrate that the formation of a mesophase is associated with a large (282 meV) hypsochromic shift only for **1[10]b**. In contrast, all other compounds that contain sulfur atoms exhibit a modest bathochromic shift of the lowest energy absorption maximum. For instance, in the all-sulfur analogue **1[10]a**, the shift is 26 nm (82 meV) and is the largest among the 5 compounds. The smallest, nearly negligible bathochromic shift of 3 nm was measured for **1[10]d**. Considering that only **1[10]b** forms a $Col_{h(o)}$ ordered phase in the series, the hypsochromic shift is associated with tight packing of molecules in the column, which is absent in other members of the series.

X-ray diffraction

XRD analysis confirmed the existence of columnar hexagonal phases in all unsymmetric derivatives **1[10]**. The liquid crystalline character of these phases is evidenced by diffused signals in

Table 2 Lowest energy absorption maxima recorded for neat samples of **1[10]** in the isotropic (Iso) and columnar phases (Col)[a]

				λ_{max}/nm	λ_{max}/nm	
1[10]	X	Y	Z	Iso	Col_h	$\Delta\lambda_{max}$/nm
a[b]	S	S	S	614	640[b]	+26
b[c]	O	O	O	630	552	−78[c]
c	O	O	S	631	644	+13
d	O	S	O	618	621	+3
e	S	S	O	612	624	+12
f	S	O	S	629	636	+7

[a] Recorded in the transmission mode. [b] Shoulder. [c] Ref. 3.

a wide-angle range, originating from short-range positional correlations between neighboring molecules along the column axis (Fig. 7). The diffractogram of **1[10]c** with a single 3,4,5-tri(decylsulfanyl)phenyl group in the N(1) position consists of two sharp signals in the small angle range and diffused halo at high angles. Such a pattern can be attributed to a Col_h phase having 2D hexagonal lattice of disordered columns, *i.e.* with liquid like order of molecules along columns (Table 3).

The high temperature phase of **1[10]d** (Fig. 7) was also identified as a Col_h phase. In contrast, the low temperature phase of **1[10]d** gave a much richer XRD pattern, which could be

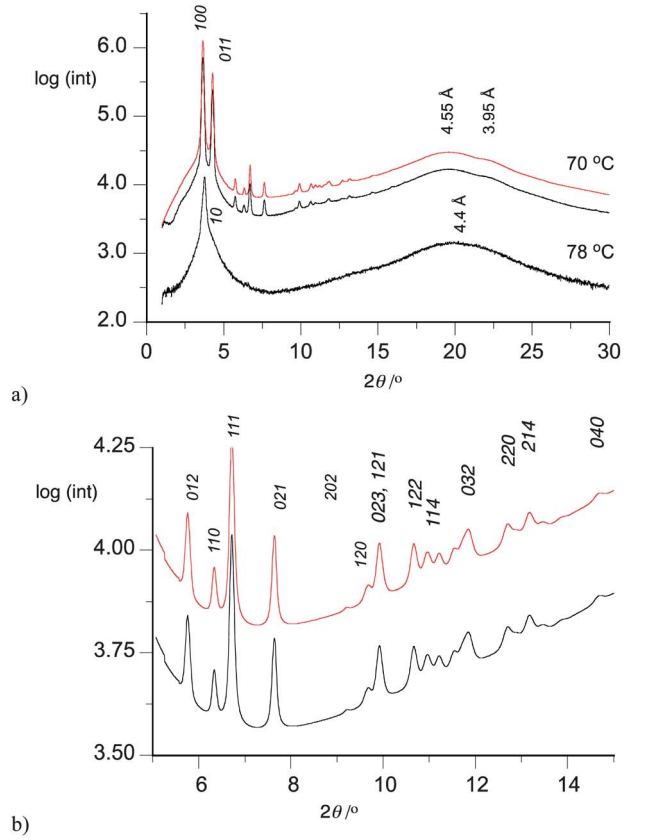

Fig. 7 XRD pattern for **1[10]d** at 70 °C with indexing for the $Col_{h(3D)}$ phase, and the high temperature phase Col_h at 78 °C. The red line represents the simulated pattern for a 3D lattice of P_6 symmetry: (a) full range pattern and (b) expansion of the mid-angle range for the $Col_{h(3D)}$ phase.

Table 3 Lattice parameters for **1[10]**

1[10]	Temp./°C	Lattice parameters (Å)	Phase
a[a]	30	$a = 27.2$, $c = 35.5$	$Col_{h(3D)}$
b[b]	110	$a = 28.95$	$Col_{h(o)}$
c	75	$a = 27.2$	Col_h
d	78	$a = 27.1$	Col_h
	70	$a = 27.9$, $c = 39.7$	$Col_{h(3D)}$
e	65	$a = 27.7$, $c = 38.2$	$Col_{h(3D)}$
f	90	$a = 28.3$, $c = 47.5$	$Col_{h(3D)}$

[a] Ref. 6. [b] Ref. 3.

indexed to a three-dimensional columnar hexagonal phase ($Col_{h(3D)}$), *i.e.* having a well defined periodicity along the columns. It should be stressed that this additional periodicity is an order of magnitude larger that the distance between neighboring molecules along the column axis, and that the positional correlations between neighboring molecules remains short-range (the phase is of disordered type). The diffused wide angle XRD signal in the $Col_{h(3D)}$ phase is split into two, reflecting a slightly different mean spacing between mesogenic cores and alkyl tails. The 3D columnar hexagonal phase was also identified from XRD patterns for the two remaining derivatives **1[10]e** and **1[10]f**.

The hexagonal lattice parameter a, related to the inter-columnar distance, is similar in both columnar phases of **1[10]d** (Table 3) indicating very little structural reorganization during the $Col_h \rightarrow Col_{h(3D)}$ phase transition. The $Col_{h(3D)}$ phase has a small thermal expansion coefficient, and both lattice parameters a and c increase only by 0.12 Å and 0.05 Å, respectively, upon cooling by 33 K.

Analysis of the data in Table 3 indicates that the lattice parameter a is similar for all six derivatives and in a range of 27–29 Å with the largest intercolumnar separation found for **1[10]b** (28.95 Å). In contrast, periodicity along the column (parameter c) varies significantly in the series and correlates with the $Col_{h(3D)}$ phase stability (Fig. 8). Thus, the largest value c was found for compound **1[10]f**, which shows the highest $Col_{h(3D)}$–I transition temperature.

A possible representation of the proposed $Col_{h(3D)}$ phase is a helical structure within the column resulting from rotation of

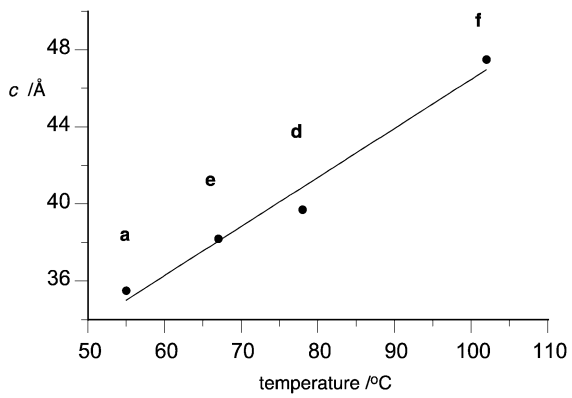

Fig. 8 A correlation between the $Col_{h(3D)}$–I ($Col_{h(3D)}$–Col_h for **1[10]d**) transition temperature and the lattice parameter c for **1[10]**.

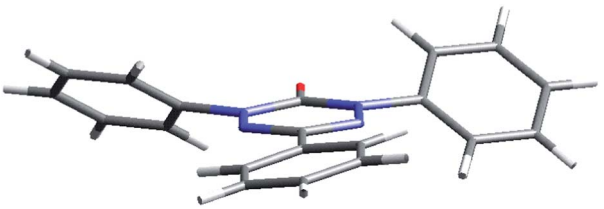

Fig. 9 B3LYP/6-31G(2d,p) optimized geometry for **7** with the imposed C_2 symmetry.

molecules along the column axis, with the periodicity of about 40 Å. This would correspond to about 10 molecules per period with each twisted relative to its neighbor by an average of about 36 degrees. Such helical structures have been observed in ordered $Col_{h(o)}$ phases of other achiral compounds that include triphenylene[12] and hexabenzocoronene[13] derivatives, in which molecules are rotated by about 45° and 20°, respectively, relative to their neighbors. The origin of this twist in **1[*n*]** might be a dipolar and/or steric interaction. DFT calculations for the parent C_2-symmetric[14] 1,3,5-triphenyl-6-oxoverdazyl (**7**, Fig. 9) give a net dipole moment of 0.77 D aligned with the C═O group, while in **1[1]a** and **1[1]b** the net dipole moment is larger and at a steep angle to the verdazyl ring plane due to the contribution form RS and RO group dipoles. The steric reason for the helical structure appears to be more plausible due to the symmetry of the molecule: the phenyl groups at the N(1) and N(5) positions are twisted (~35°) relative to the verdazyl ring in the conformational ground state. This twist, giving rise to a propeller-like structure, may impose the helical arrangement of the molecules within the column. Interestingly, contrary to previous reports,[12,13] well-defined, long periodicity along the column was observed for disordered columnar hexagonal phases (Col_h) in **1[10]**, but not for the ordered type $Col_{h(o)}$ phase exhibited by **1[10]b**.

Magnetic and photovoltaic characterization

Magnetic studies of **1[10]d** at 500 Oe revealed nearly ideal paramagnetic behavior in both the liquid crystalline and isotropic phases. Similar to previous observations for **1[8]a**, no abrupt changes were detected upon phase transitions, which indicates that the spins are isolated in both phases.[2] In contrast, a sample of **1[8]b** showed a small decrease of magnetization upon isotropic to mesophase transition.[3]

Time-of-Flight (ToF) studies of an unaligned sample of **1[10]d** in cells of 12.5 μm or 4.75 μm gap (applied voltage of 30–50 kV cm^{-1}) showed only a negligible transient photocurrent in the range of 80–30 °C that was insufficient to calculate charge mobility. In the case of **1[8]a** and **1[8]b** also weak photocurrent was detected and hole mobility μ_h was calculated to be about 3×10^{-3} cm^2 V^{-1} s^{-1} in the mesophase.[2,3] No photocurrent was detected in the isotropic phase of the latter compound.

Conclusions

A gradual replacement of the oxygen atoms in the decyloxy derivative **1[10]b** with sulfur atoms leads to change of columnar hexagonal phase organization from ordered ($Col_{h(o)}$) to disordered (Col_h) to 3 dimensional ($Col_{h(3D)}$). The $Col_{h(3D)}$ phase is more organized than the Col_h phase, as evident from the phase sequence in **1[10]d**. Spectroscopic investigation of series **1[10]** revealed that only all-decyloxy derivative **1[10]b** exhibit hypsothermochromism, which is associated with the tight molecular packing in the ordered $Col_{h(o)}$ phase. Detailed studies of **1[10]d** demonstrated essentially isolated spins in all phases, and negligible photocurrent due to efficient charge traps.

Computational details

Quantum-mechanical calculations were carried out at the UB3LYP/6-31G(d,p) level of theory using the Gaussian 09 suite of programs.[15] Geometry optimizations were undertaken using default convergence limits and without symmetry constraints. No conformational search for the global minimum was attempted.

Electronic excitation energies for **1[1]** in a vacuum were obtained at the UB3LYP/6-31G(d,p) level using the time-dependent DFT method[16] supplied in the Gaussian package.

Experimental part

General

^{1}H NMR spectra were obtained at 400 MHz (^{1}H) in $CDCl_3$ and referenced to the solvent unless stated otherwise. Thermal analysis was performed on a TA 2920 DSC using a typical heating rate of 5 K min^{-1}. Reactions were carried out under Ar, and subsequent manipulations were conducted in air. Details of magnetization and photoconductivity measurements were described previously.[3]

Electronic absorption spectra

UV-vis spectra for **1[8]b** were recorded in spectroscopic grade hexane at a concentration of 1–10 × 10^{-6} M. Extinction coefficients were obtained by fitting the maximum absorbance at 260 or 261 nm against the concentration in agreement with Beer's law.

Visible spectra for neat **1[10]** placed between two glass slides were obtained at temperatures about 10 K above and then 10 K below the Col–I phase transition for each compound using a hot-stage mounted in a UV spectrometer. For **1[10]d** the spectrum of the Col_h phase was recorded in the middle of the phase range.

6-Oxoverdazyls 1[10]

General procedure. To a solution of carbamoyl chloride **5[10]**[10] (1.0 mmol) in dry benzene (30 mL) a solution of freshly prepared 3,4,5-tridecyloxyphenylhydrazine[8] or 3,4,5-tridecylsulfanylphenylhydrazine[8] (**2[10]**, 1.2 mmol) and Et_3N (1.3 mmol) in dry benzene (10 mL) was added. The mixture was stirred for 2 h at 50 °C. A 1% solution of HCl was added, organic products were extracted (CH_2Cl_2), extracts were dried (Na_2SO_4), and solvents were evaporated. The residue was passed through a short silica gel column (hexane–CH_2Cl_2, 2 : 1) to give a fraction containing tetrazine **6[10]** identified by characteristic signals in the ^{1}H NMR: δ 4.71 (d, J = 8.5 Hz, 2H) and 5.46 (t, J = 8.5 Hz, 1H).

A mixture of partially purified tetrazine **6[10]** (0.1 mmol), anhydrous Na_2CO_3 (106 mg, 1.0 mmol), PbO_2 (478 mg, 2.0 mmol) in a mixture of toluene (6 mL) and MeCN (1.5 mL) was stirred overnight at rt. The dark reaction mixture was passed through a silica gel plug (CH_2Cl_2), and the crude product was purified on a silica gel column (hexane–CH_2Cl_2, 6 : 1) to give radical **1[10]** as a dark blue waxy solid in overall yields of about 35% based on **5[10]**. The solid was recrystallized several times from AcOEt or AcOEt with a few drops of MeCN at −78 °C.

1,3,-Di-(3,4,5-tridecyloxyphenyl)-5-(3,4,5-tridecylsulfanylphenyl)-6-oxoverdazyl (1[10]c)

UV (hexane) λ_{max} (log ε) 618 (3.55), 497 (3.34), 359 (3.98), 290 sh (4.41), 260 (4.62) nm. Anal. calcd for $C_{110}H_{195}N_4O_7S_3$: C, 74.14; H, 11.03; N, 3.14. Found: C, 74.27; H, 10.95; N, 3.14%.

1,5,-Di-(3,4,5-tridecyloxyphenyl)-3-(3,4,5-tridecylsulfanylphenyl)-6-oxoverdazyl (1[10]d)

UV (hexane) λ_{max} (log ε) 609 (3.67), 495 (3.56), 340 (4.23), 261 (4.68) nm. Anal. calcd for $C_{110}H_{195}N_4O_7S_3$: C, 74.14; H, 11.03; N, 3.14. Found: C, 74.25; H, 10.96; N, 3.11%.

1,3,-Di-(3,4,5-tridecylsulfanylphenyl)-5-(3,4,5-tridecyloxyphenyl)-6-oxoverdazyl (1[10]e)

UV (hexane) λ_{max} (log ε) 609 (3.60), 507 (3.44), 362 sh (3.95), 3.27 (4.21), 261 (4.83) nm. Anal. calcd for $C_{110}H_{195}N_4O_4S_6$: C, 72.19; H, 10.74; N, 3.06. Found: C, 72.44; H, 10.69; N, 3.04%.

1,5,-Di-(3,4,5-tridecylsulfanylphenyl)-3-(3,4,5-tridecyloxyphenyl)-6-oxoverdazyl (1[10]f)

UV (hexane) λ_{max} (log ε) 620 (3.59), 510 (3.42), 367 (4.09), 325 (4.18), 291 sh (4.52), 260 (4.81), 222 sh (4.75) nm. Anal. calcd for $C_{110}H_{195}N_4O_4S_6$: C, 72.19; H, 10.74; N, 3.06. Found: C, 72.11; H, 10.69; N, 2.94%.

Acknowledgements

This work was supported by NSF grants (CHEM-1214104). We thank Prof. Andrzej Twardowski for funding SQUID measurements.

References

1 P. Kaszynski, in *Magnetic Properties of Organic Materials*, ed. P. M. Lahti, Marcel Dekker, New York, 1999, p. 305.
2 A. Jankowiak, D. Pociecha, J. Szczytko, H. Monobe and P. Kaszyński, *J. Am. Chem. Soc.*, 2012, **134**, 2465.
3 A. Jankowiak, D. Pociecha, H. Monobe, J. Szczytko and P. Kaszyński, *Chem. Commun.*, 2012, **48**, 7064.
4 A. Jankowiak, D. Pociecha, H. Monobe, J. Szczytko, Z. Debska, J. Romanski and P. Kaszyński, *Phosphorus, Sulfur Silicon Relat. Elem.*, 2013, **188**, 418.
5 S. Castellanos, F. López-Calahorra, E. Brillas, L. Juliá and D. Velasco, *Angew. Chem., Int. Ed.*, 2009, **48**, 6516.
6 A. Jankowiak, D. Pociecha, J. Szczytko, H. Monobe and P. Kaszyński, *Liq. Cryst.*, 2014, **41**, DOI: 10.1080/02678292.2013.828334.
7 R. Milcent, G. Barbier, S. Capelle and J.-P. Catteau, *J. Heterocycl. Chem.*, 1994, **31**, 319.
8 A. Jankowiak and P. Kaszyński, *Beilstein J. Org. Chem.*, 2012, **8**, 275.
9 A. Jankowiak, Z. Dębska, P. Kaszyński and J. Romański, *J. Sulfur Chem.*, 2012, **33**, 1.
10 For details see ESI.†
11 R. G. Hicks, in *Stable Radicals: Fundamentals and Applied Aspects of Odd-Electron Compounds*, ed. R. G. Hicks, Wiley & Sons, 2010, pp. 245–280, and references therein.
12 E. Fontes, P. A. Heiney and W. H. de Jeu, *Phys. Rev. Lett.*, 1988, **61**, 1202.
13 W. Pisula, Ž. Tomović, M. D. Watson and K. Müllen, *J. Phys. Chem. B*, 2007, **111**, 7481.
14 The C_s symmetric derivative **7** has essentially the same enthalpy of formation. The experimental structure of **7** also has C_2 symmetry: F. A. Neugebauer, H. Fischer and C. Krieger, *J. Chem. Soc., Perkin Trans. 2*, 1993, 535.
15 M. J. Frisch, G. W. Trucks, H. B. Schlegel, G. E. Scuseria, M. A. Robb, J. R. Cheeseman, G. Scalmani, V. Barone, B. Mennucci, G. A. Petersson, H. Nakatsuji, M. Caricato, X. Li, H. P. Hratchian, A. F. Izmaylov, J. Bloino, G. Zheng, J. L. Sonnenberg, M. Hada, M. Ehara, K. Toyota, R. Fukuda, J. Hasegawa, M. Ishida, T. Nakajima, Y. Honda, O. Kitao, H. Nakai, T. Vreven, J. A. Montgomery, Jr, J. E. Peralta, F. Ogliaro, M. Bearpark, J. J. Heyd, E. Brothers, K. N. Kudin, V. N. Staroverov, R. Kobayashi, J. Normand, K. Raghavachari, A. Rendell, J. C. Burant, S. S. Iyengar, J. Tomasi, M. Cossi, N. Rega, J. M. Millam, M. Klene, J. E. Knox, J. B. Cross, V. Bakken, C. Adamo, J. Jaramillo, R. Gomperts, R. E. Stratmann, O. Yazyev, A. J. Austin, R. Cammi, C. Pomelli, J. W. Ochterski, R. L. Martin, K. Morokuma, V. G. Zakrzewski, G. A. Voth, P. Salvador, J. J. Dannenberg, S. Dapprich, A. D. Daniels, O. Farkas, J. B. Foresman, J. V. Ortiz, J. Cioslowski and D. J. Fox, *Gaussian 09, Revision A.02*, Gaussian, Inc., Wallingford CT, 2009.
16 R. E. Stratmann, G. E. Scuseria and M. J. Frisch, *J. Chem. Phys.*, 1998, **109**, 8218.

